SUPPLEMENTARY INFORMATION

Spatially organized tumor-stroma boundary determines the efficacy of immunotherapy in colorectal cancer patients

Yu Feng[1,2,3,4*], Wenjuan Ma[5,6*], Yupeng Zang[7], Yanying Guo[2], Young Li[1,2], Yixuan Zhang[8], Xuan Dong[2], Yi Liu[2,7], Xiaojuan Zhan[2,7], Zhizhong Pan[5,9], Mei Luo[2,7], Miaoqing Wu[5,9], Ao Chen[1,2], Da Kang[5,9], Gong Chen[5,9#], Longqi Liu[1,2,4#], Jingying Zhou[8#], Rongxin Zhang[5,9,10#]

[1]BGI Research, Shenzhen 518083, China.

[2]BGI Research, Hangzhou 310030, China.

[3]Guangdong Provincial Key Laboratory of Human Disease Genomics, Shenzhen Key Laboratory of Genomics, BGI Research, Shenzhen 519083, China.

[4]Shanxi Medical University - BGI Collaborative Center for Future Medicine, Shanxi Medical University, Taiyuan 030605, China

[5]State Key Laboratory of Oncology in South China, Guangzhou 510060, Guangdong, People's Republic of China.

[6]Department of Intensive Care Unit, Sun Yat-sen University Cancer Centre, Guangzhou 510060, Guangdong, People's Republic of China.

[7]College of Life Sciences, University of Chinese Academy of Sciences, Beijing 100049, China.

[8]School of Biomedical Sciences, The Chinese University of Hong Kong, Hong Kong SAR, 999077, China.

[9]Department of Colorectal Surgery, Sun Yat-sen University Cancer Centre, Guangzhou 510060, Guangdong, People's Republic of China

[10]Lead Contact

*These authors contributed equally to this work

Correspondence:

Gong Chen, Department of Colorectal Surgery, Sun Yat-sen University Cancer Centre, State Key Laboratory of Oncology in South China, Guangzhou, Guangdong, 510060, P. R. China. TEL: +86 20 87343584; FAX: +86 20 87343584; EMAIL: chengong@sysucc.org.cn

Longqi Liu, BGI Research Hangzhou, Hangzhou, 310030, P. R. China. TEL: +86 0571 88226065; EMAIL: liulongqi@genomics.cn

Jingying Zhou, School of Biomedical Sciences, The Chinese University of Hong Kong, Hong Kong SAR, 999077, P.R. China. TEL: +852 39431350; FAX: +852 26035139; EMAIL: zhoujy@cuhk.edu.hk

Rongxin Zhang, Department of Colorectal Surgery, Sun Yat-sen University Cancer Centre, State Key Laboratory of Oncology in South China, Guangzhou, Guangdong, 510060, P. R. China. TEL: +86 20 87343584; FAX: +86 20 87343584; EMAIL: zhangrx@sysucc.org.cn

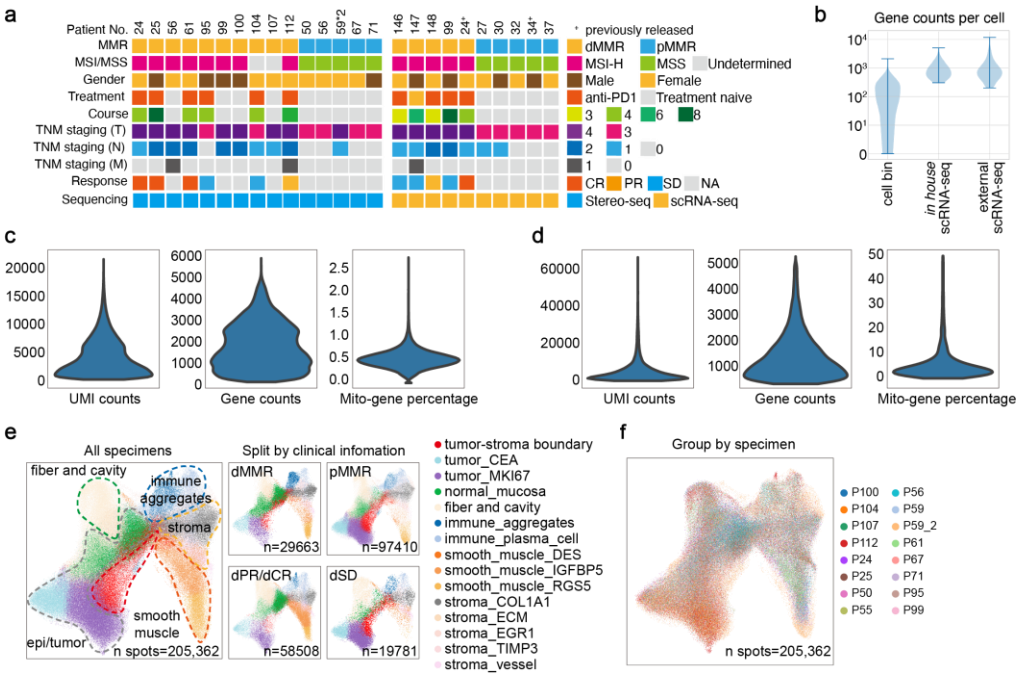

Supplementary Figure 1. ***Basic information of the Stereo-seq data.***

a Matrix plots of the clinical informations of our CRC patient cohort are shown. **b** Violin plots of the gene counts per cell in cell bin segmented of Stereo-seq data from a representative patient #59, our in house scRNA-seq data and a representative public scRNA-seq data (GSE178341) are shown. **c** Violin plots of unique molecular identifier (UMI) counts, gene counts and mitochondria-related (Mito-gene) genes percentage in the Stereo-seq, or **d** scRNAseq data are shown. **e** UMAP of the spatial transcriptome data from 205,362 bin spots from 15 CRC patients are shown. Bins are colored by spatial cell clusters, split by clinical information or **f** colored by patient ID.

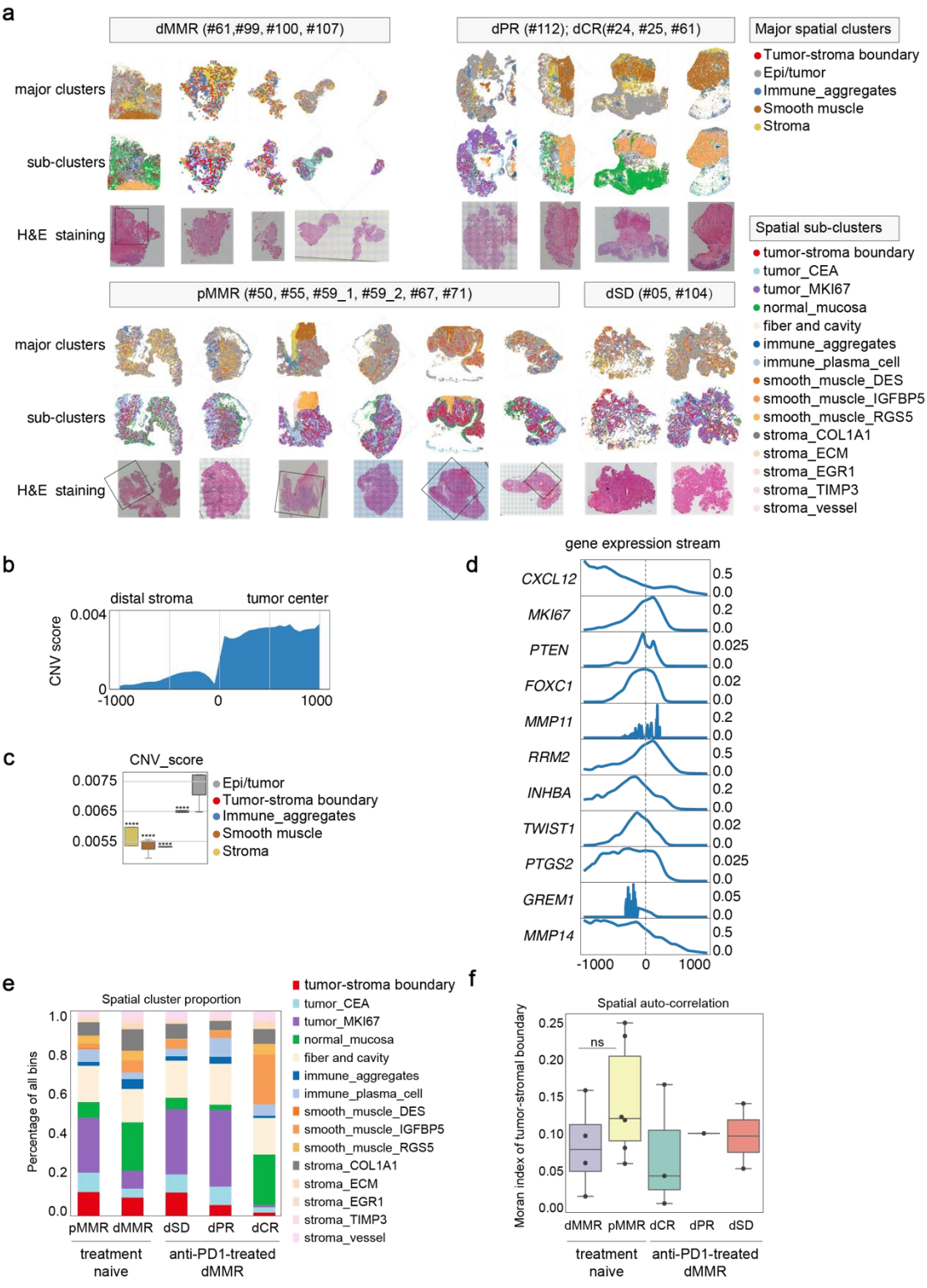
a
dMMR (#61,#99, #100, #107)
dPR (#112); dCR(#24, #25, #61)
Major spatial clusters
Tumor-stroma boundary
Epi/tumor
Immune_aggregates
Smooth muscle
Stroma
major clusters
sub-clusters
H&E staining
Spatial sub-clusters
tumor-stroma boundary
tumor_CEA
tumor_MKI67
normal_mucosa
fiber and cavity
immune_aggregates
immune_plasma_cell
smooth_muscle_DES
smooth_muscle_IGFBP5
smooth_muscle_RGS5
stroma_COL1A1
stroma_ECM
stroma_EGR1
stroma_TIMP3
stroma_vessel
pMMR (#50, #55, #59_1, #59_2, #67, #71)
dSD (#05, #104)
b
distal stroma
tumor center
CNV score
0.004
0
-1000
0
1000
c
CNV_score
0.0075
0.0065
0.0055
Epi/tumor
Tumor-stroma boundary
Immune_aggregates
Smooth muscle
Stroma
d
gene expression stream
CXCL12
MKI67
PTEN
FOXC1
MMP11
RRM2
INHBA
TWIST1
PTGS2
GREM1
MMP14
0.5
0.0
0.2
0.0
0.025
0.0
0.02
0.0
0.2
0.0
0.5
0.0
0.2
0.0
0.02
0.0
0.025
0.0
0.05
0.0
0.5
0.0
-1000
0
1000
e
Spatial cluster proportion
Percentage of all bins
1.0
0.8
0.6
0.4
0.2
0.0
pMMR
dMMR
dSD
dPR
dCR
treatment naive
anti-PD1-treated dMMR
tumor-stroma boundary
tumor_CEA
tumor_MKI67
normal_mucosa
fiber and cavity
immune_aggregates
immune_plasma_cell
smooth_muscle_DES
smooth_muscle_IGFBP5
smooth_muscle_RGS5
stroma_COL1A1
stroma_ECM
stroma_EGR1
stroma_TIMP3
stroma_vessel
f
Spatial auto-correlation
Moran index of tumor-stromal boundary
ns
0.25
0.20
0.15
0.10
0.05
0.00
dMMR
pMMR
dCR
dPR
dSD
treatment naive
anti-PD1-treated dMMR

Supplementary Figure 2. ***Global landscape of spatial cell clusters***

a The spatial plots of the major spatial clusters, sub-clusters and H&E image in each specimen are shown. **b** The stacked stream plot of the CNV scores from the distal stroma (-1000μm, left) to the tumor center (1000μm, right) is shown. The mean CNV score in each 1mm interval is smoothed using slinger model. The distance of boundary was set to 0μm. **c** The box-whisker plots of the CNV scores in each major spatial cluster are shown (n spots: Epi/tumor=82,655, tumor-stroma boundary=17,639, immune aggregates=16,304, smooth muscle=24,172, stroma=28,012). The asterisk represents the comparison of the epi/tumor clusters towards other spatial clusters, analyzed by two-tailed unpaired Student-t test with Bonferroni correction. ****, $p<0.0001$. Data are represented mean±IQR (25%~75%) with minima (lower bar) and maxima (upper bar). **d** The stacked stream plots of the indicated gene expressions from the distal stroma (-1000μm, left) to the tumor center (1000μm, right) are shown. The mean expression level in each 1mm interval is smoothed using slinger model. The distance of boundary was set to 0μm. **e** Stacked box plots show the proportions of spatial clusters in the indicated patient groups. **f** Spatial auto-correlation of tumor-stroma boundary is shown by Moran index. Data are represented mean±IQR (25%~75%) with minima (lower bar) and maxima (upper bar). Statistics are analyzed by two-tailed unpaired Student-t test with Bonferroni correction. ns, not significant. N number of the patients: pMMR=6; dMMR=4; dSD=2; dPR=1; dCR=3.

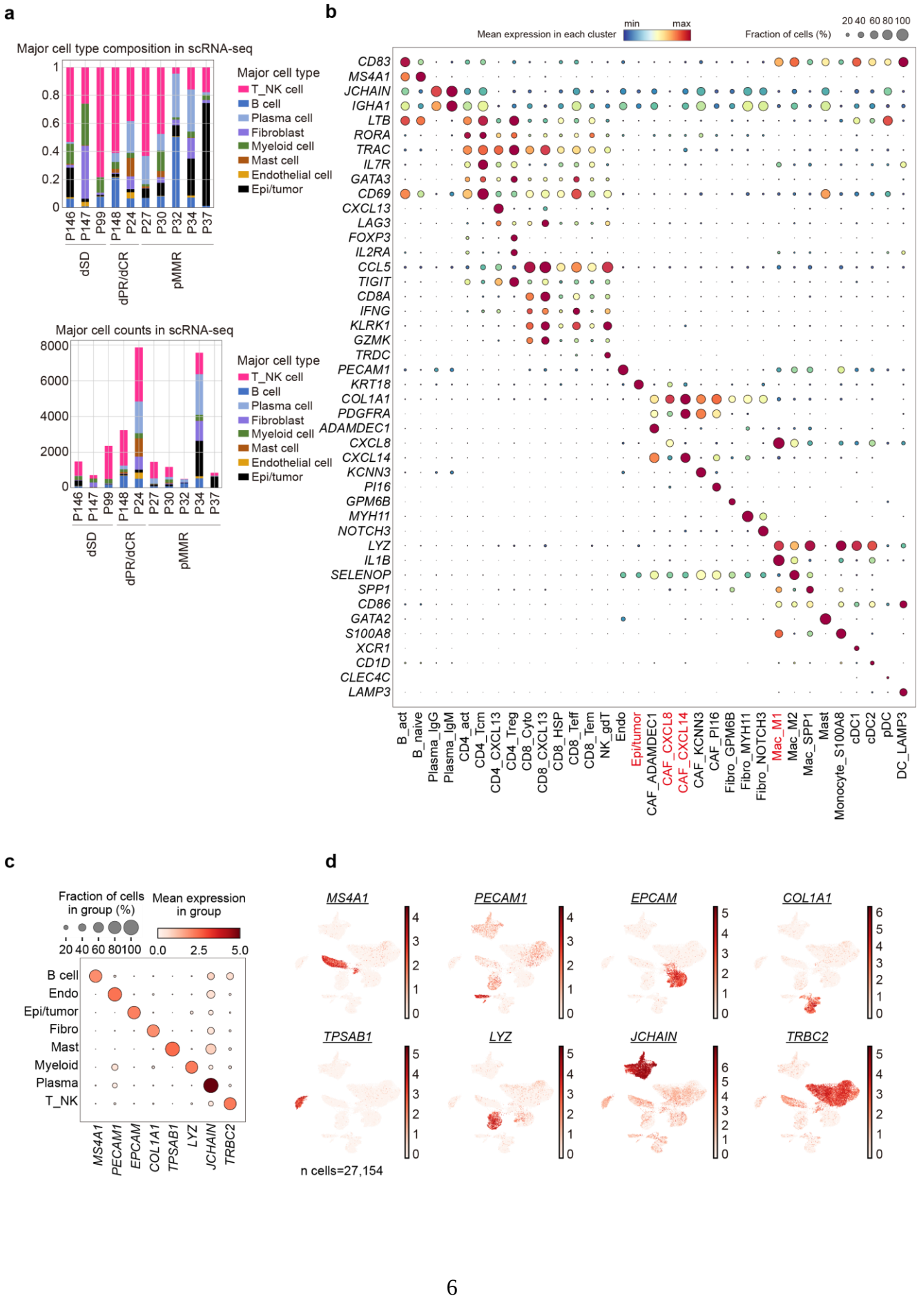
a
Major cell type composition in scRNA-seq
Major cell type
T_NK cell
B cell
Plasma cell
Fibroblast
Myeloid cell
Mast cell
Endothelial cell
Epi/tumor
P146 P147 P99 P148 P24 P27 P30 P32 P34 P37
dSD
dPR/dCR
pMMR
Major cell counts in scRNA-seq
b
Mean expression in each cluster
min
max
Fraction of cells (%)
20 40 60 80 100
CD83 MS4A1 JCHAIN IGHA1 LTB RORA TRAC IL7R GATA3 CD69 CXCL13 LAG3 FOXP3 IL2RA CCL5 TIGIT CD8A IFNG KLRK1 GZMK TRDC PECAM1 KRT18 COL1A1 PDGFRA ADAMDEC1 CXCL8 CXCL14 KCNN3 PI16 GPM6B MYH11 NOTCH3 LYZ IL1B SELENOP SPP1 CD86 GATA2 S100A8 XCR1 CD1D CLEC4C LAMP3
B_act B_naive Plasma_IgG Plasma_IgM CD4_act CD4_Tcm CD4_CXCL13 CD4_Treg CD8_Cyto CD8_CXCL13 CD8_HSP CD8_Teff CD8_Tem NK_gdT Endo Epi/tumor CAF_ADAMDEC1 CAF_CXCL8 CAF_CXCL14 CAF_KCNN3 CAF_PI16 Fibro_GPM6B Fibro_MYH11 Fibro_NOTCH3 Mac_M1 Mac_M2 Mac_SPP1 Mast Monocyte_S100A8 cDC1 cDC2 pDC DC_LAMP3
c
Fraction of cells in group (%)
Mean expression in group
20 40 60 80 100
0.0 2.5 5.0
B cell Endo Epi/tumor Fibro Mast Myeloid Plasma T_NK
MS4A1 PECAM1 EPCAM COL1A1 TPSAB1 LYZ JCHAIN TRBC2
d
MS4A1 PECAM1 EPCAM COL1A1
TPSAB1 LYZ JCHAIN TRBC2
n cells=27,154

Supplementary Figure 3. ***Basic information of the scRNA-seq data.***

a The stacked bar plots of proportions or absolute cell counts of the major cell clusters in the scRNA-seq data of each patients are shown. **b** Bubble plots of marker gene expressions in all cell clusters or **c** major cell clusters from the scRNA-seq dataset are shown. The plots are sized by the fraction of cells with positive gene expression, while the color represents the gene expression level. **d** Expression level of canonical marker genes for each major cell cluster is shown in UMAP (n cells=27,154; n samples: 5 pMMR, 2 dPR/CR, 3 dSD).

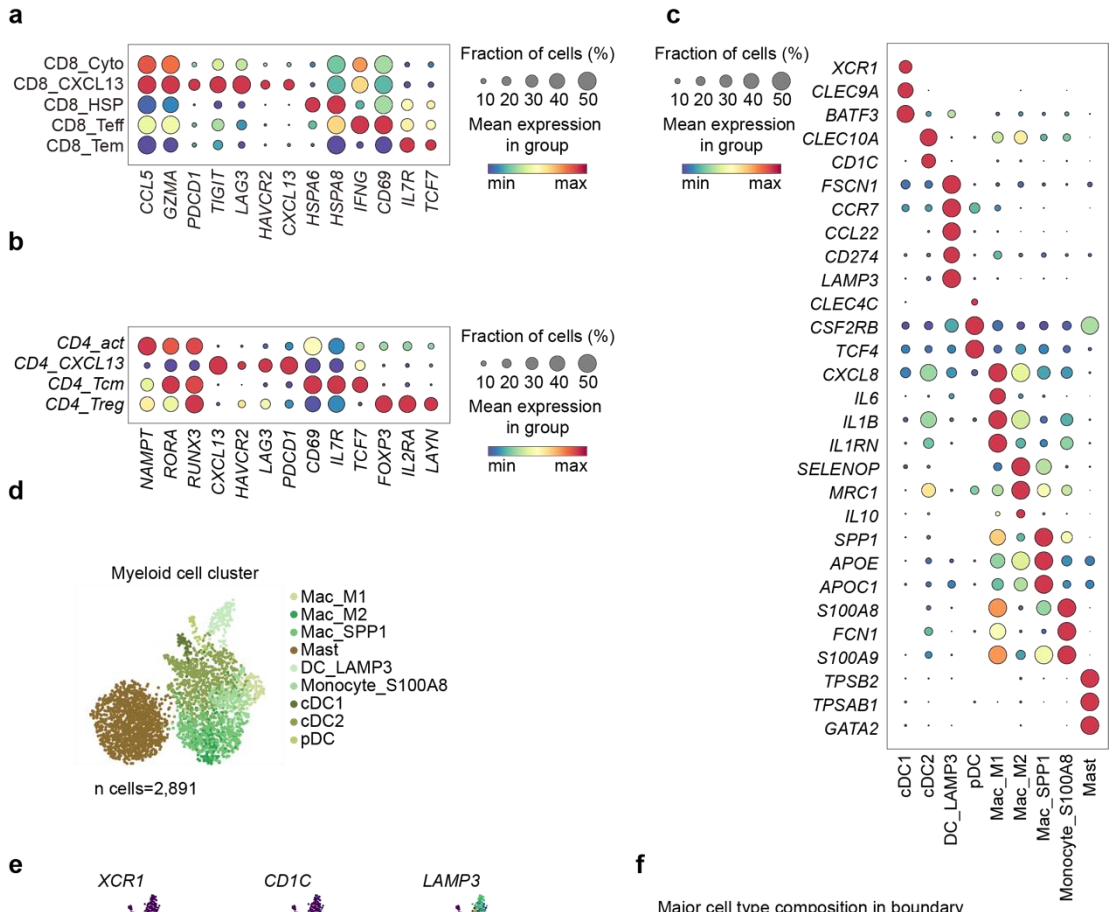
a
CD8_Cyto
CD8_CXCL13
CD8_HSP
CD8_Teff
CD8_Tem
CCL5 GZMA PDCD1 TIGIT LAG3 HAVCR2 CXCL13 HSPA6 HSPA8 IFNG CD69 IL7R TCF7
Fraction of cells (%)
10 20 30 40 50
Mean expression in group
min max
b
CD4_act
CD4_CXCL13
CD4_Tcm
CD4_Treg
NAMPT RORA RUNX3 CXCL13 HAVCR2 LAG3 PDCD1 CD69 IL7R TCF7 FOXP3 IL2RA LAYN
Fraction of cells (%)
10 20 30 40 50
Mean expression in group
min max
c
Fraction of cells (%)
10 20 30 40 50
Mean expression in group
min max
XCR1 CLEC9A BATF3 CLEC10A CD1C FSCN1 CCR7 CCL22 CD274 LAMP3 CLEC4C CSF2RB TCF4 CXCL8 IL6 IL1B IL1RN SELENOP MRC1 IL10 SPP1 APOE APOC1 S100A8 FCN1 S100A9 TPSB2 TPSAB1 GATA2
cDC1 cDC2 DC_LAMP3 pDC Mac_M1 Mac_M2 Mac_SPP1 Monocyte_S100A8 Mast
d
Myeloid cell cluster
Mac_M1
Mac_M2
Mac_SPP1
Mast
DC_LAMP3
Monocyte_S100A8
cDC1
cDC2
pDC
n cells=2,891
e
XCR1 CD1C LAMP3
TCF4 S100A8 IL6
MRC1 SPP1 TPSB2
max
min
n cells=2,891
f
Major cell type composition in boundary
Fraction of cells
1.0 0.8 0.6 0.4 0.2 0.0
T_NK
Bcell
Plasma
Fibro
Myeloid
Mast
Endo
Epi/tumor
P56 P99 P100 P107 P50 P55 P59 P59_2 P67 P71 P24 P25 P61 P112 P95 P104
dMMR pMMR dPR/dCR dSD
g
dMMR
dPR/dCR
pMMR
dSD
RCTD frequencies (centered to 0)
0.15 0.00 -0.15
-1000 -500 0 500 1000
Major cell clusters
T_NK cell
B cell
Plasma cell
Myeloid cell
Mast cell

Supplementary Figure 4. ***Characterization of T cell and myeloid cell clusters.***

a Bubble plots of marker gene expressions in $CD8^+$T cells, **b** $CD4^+$T cells, and **c** myeloid cells from the scRNA-seq dataset are shown. The plot are sized by the fraction of cells with positive gene expression, while the color represents the gene expression level. **d** UMAP of myeloid cell clusters (n cells=2,891; n samples: 5 pMMR, 2 dPR/CR, 3 dSD) and **e** expression level of canonical marker genes for each cluster are shown. **f** Stacked box plots of the proportions of major cell clusters in the tumor-stromal boundary of each patient from Stereo-seq data are shown. **g** The stacked stream plots of major immune cell distribution patterns from distal stroma (-1000μm, left) to tumor center (1000μm, right) in indicated patient groups are shown. The mean RCTD frequencies of each immune cell in each 1mm interval was smoothed using slinger model and colored by cell clusters in accordance with **Fig. 2b**.

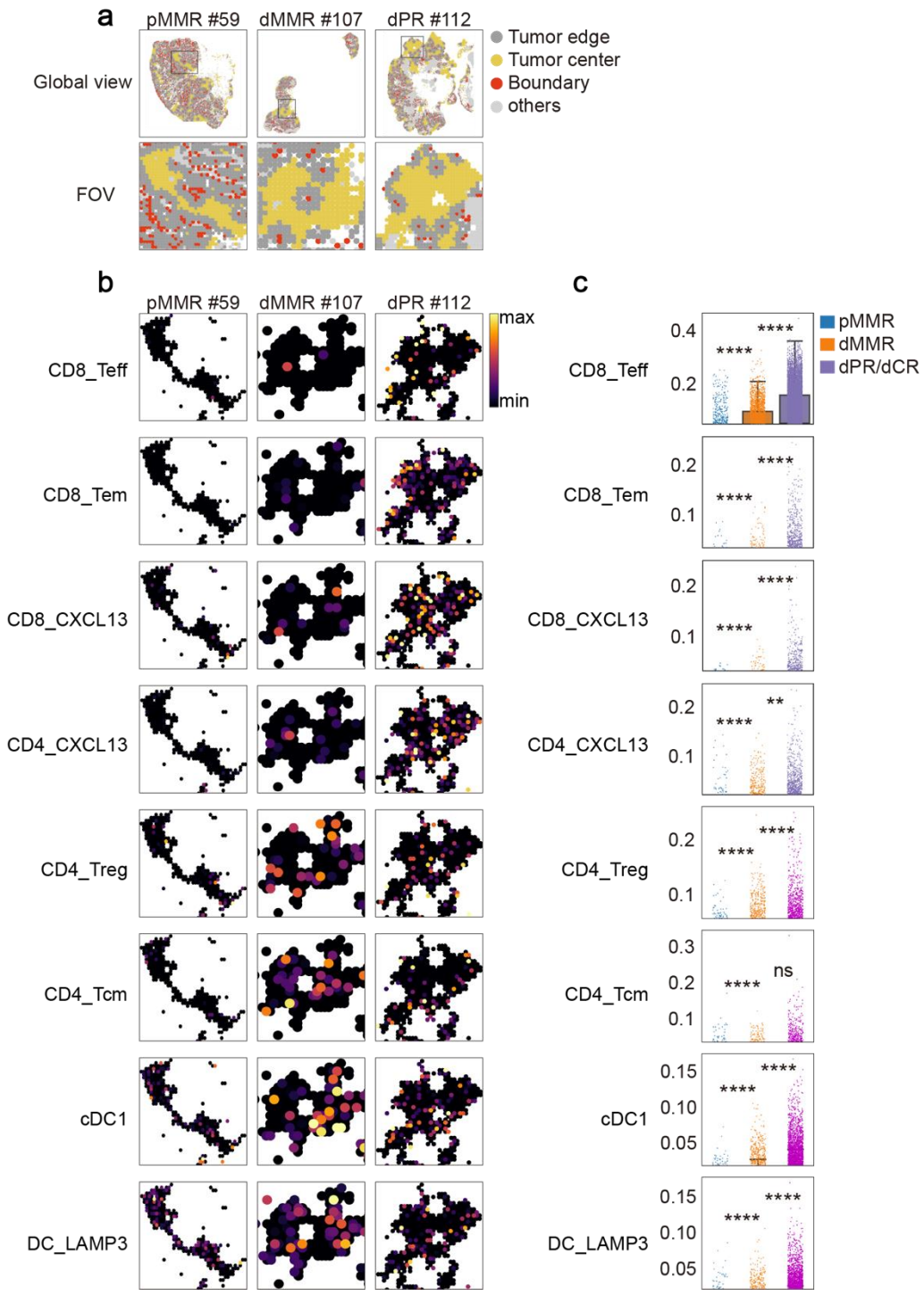

Supplementary Figure 5. ***The distributions of immune cell clusters in the spatial map.***

a Representative images of overviewed FOVs and **b** indicated immune cell clusters in the spatial map of pMMR patient #59, dMMR patient #107 and dPR patient #112 are shown. **c** The RCTD frequencies of indicated immune cell clusters are shown in dot

plot graphs in indicated patient groups. Data are represented as box-whisker plot (mean±IQR: 25%~75%) and analyzed by two-tailed unpaired Student-t test with Bonferroni correction. ns, not significant; **, $p<0.01$; ****, $p<0.0001$. N spots: pMMR=7,694; dMMR=2,595; dPR/dCR=10.283.

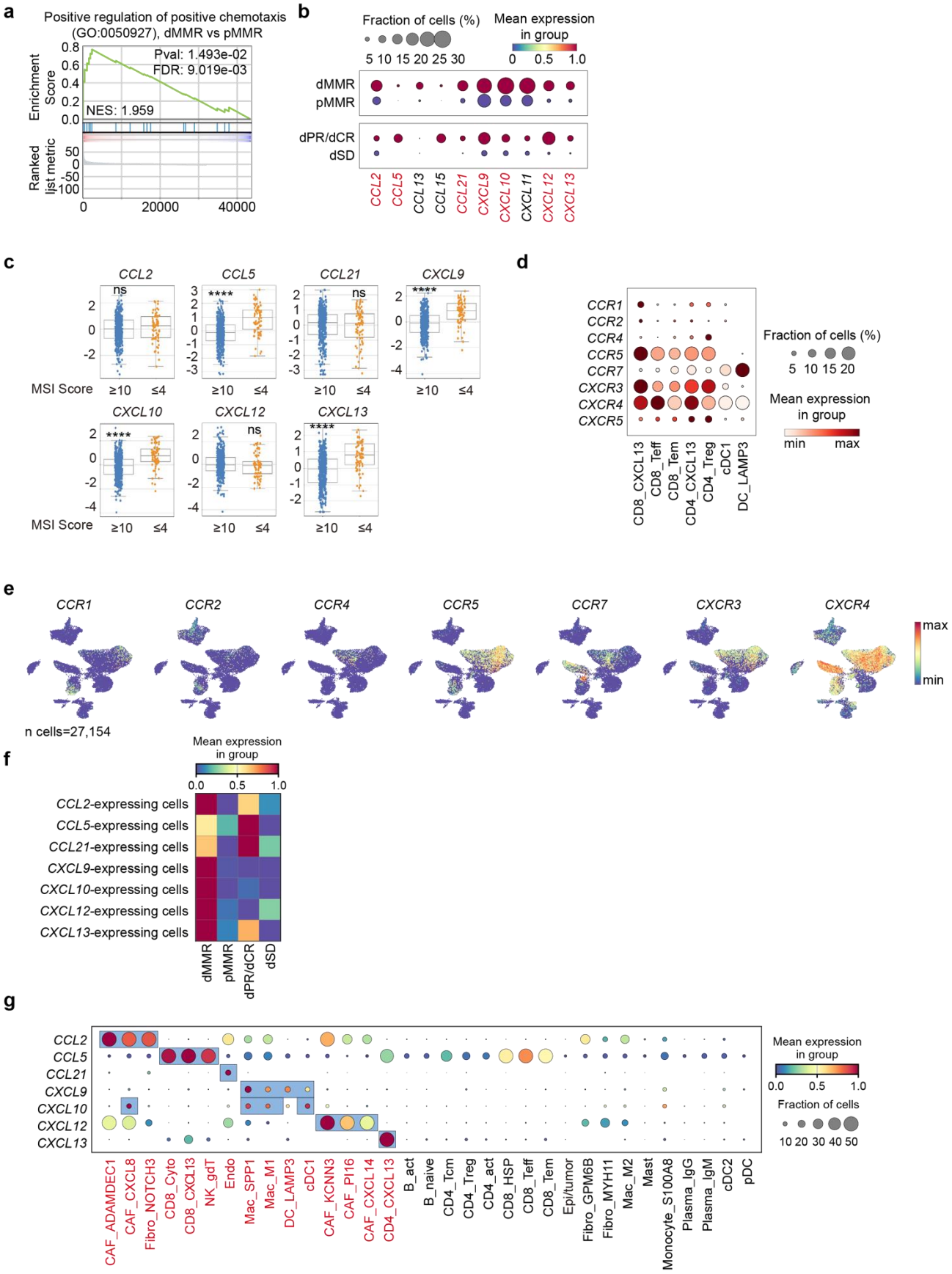
a
Positive regulation of positive chemotaxis
(GO:0050927), dMMR vs pMMR
Pval: 1.493e-02
FDR: 9.019e-03
NES: 1.959
Enrichment Score
Ranked list metric
b
Fraction of cells (%)
Mean expression in group
dMMR
pMMR
dPR/dCR
dSD
CCL2 CCL5 CCL13 CCL15 CCL21 CXCL9 CXCL10 CXCL11 CXCL12 CXCL13
c
CCL2 CCL5 CCL21 CXCL9 CXCL10 CXCL12 CXCL13
ns
****
MSI Score
≥10 ≤4
d
CCR1 CCR2 CCR4 CCR5 CCR7 CXCR3 CXCR4 CXCR5
CD8_CXCL13 CD8_Teff CD8_Tem CD4_CXCL13 CD4_Treg cDC1 DC_LAMP3
Fraction of cells (%)
Mean expression in group
min max
e
CCR1 CCR2 CCR4 CCR5 CCR7 CXCR3 CXCR4
max
min
n cells=27,154
f
Mean expression in group
CCL2-expressing cells
CCL5-expressing cells
CCL21-expressing cells
CXCL9-expressing cells
CXCL10-expressing cells
CXCL12-expressing cells
CXCL13-expressing cells
dMMR pMMR dPR/dCR dSD
g
CCL2 CCL5 CCL21 CXCL9 CXCL10 CXCL12 CXCL13
Mean expression in group
Fraction of cells
CAF_ADAMDEC1 CAF_CXCL8 Fibro_NOTCH3 CD8_Cyto CD8_CXCL13 NK_gdT Endo Mac_SPP1 Mac_M1 DC_LAMP3 cDC1 CAF_KCNN3 CAF_PI16 CAF_CXCL14 CD4_CXCL13 B_act B_naive CD4_Tcm CD4_Treg CD4_act CD8_HSP CD8_Teff CD8_Tem Epi/tumor Fibro_GPM6B Fibro_MYH11 Mac_M2 Mast Monocyte_S100A8 Plasma_IgG Plasma_IgM cDC2 pDC

Supplementary Figure 6. ***Key chemotaxis pathways in T cells and DCs from the tumor-stroma boundary of treatment naïve dMMR and anti-PD1-treated dPR/dCR patients.***

a GSEA plot of the upregulated genes related to positive regulation of positive chemotaxis (GO:0050927) in the tumor-stroma boundary of treatment naïve dMMR compared to pMMR is shown. GSEA plot showing the up-regulation of the genes related to in dMMR boundaries (in comparison to pMMR boundaries). **b** Bubble plots of indicated chemokine expressions in the tumor-stroma boundary of indicated patient groups. The plots are sized by the fraction of cells with positive gene expression, while the color represents the gene expression level. The chemokines with higher expressions in treatment naïve dMMR compared to pMMR, as well as in anti-PD1-treated dPR/dCR compared to dSD are highlighted in red. **c** The expressions of indicated chemokines from MSI-hi (MSI score≥10, n = 78 patients) and MSI-lo (MSI score≥10, n = 494 patients) groups in COAD TCGA data are shown as box-whisker plot. Data are represented mean±IQR (25%~75%) with minima (lower bar) and maxima (upper bar). Statistics are analyzed by two-tailed unpaired Student-t test with Bonferroni correction. ns, not significant; ****, $p<0.0001$. **d** Bubble plots of chemokine receptors of chemokines highlighted in **b** from indicated immune cell clusters are shown. The plots are sized by the fraction of cells with positive gene expression, while the color represents the gene expression level. **e** UMAP of indicated chemokine receptor expressions from the scRNA-seq dataset (n cells=27,154; n samples: 5 pMMR, 2 dPR/CR, 3 dSD). **f** Heatmap of chemokine-expressing cells in the tumor-stroma boundary of indicated patient groups. **g** Bubble plots of the chemokine expressions profiling in the cell clusters from the scRNA-seq dataset. The cells of interests are highlighted in red and framed.

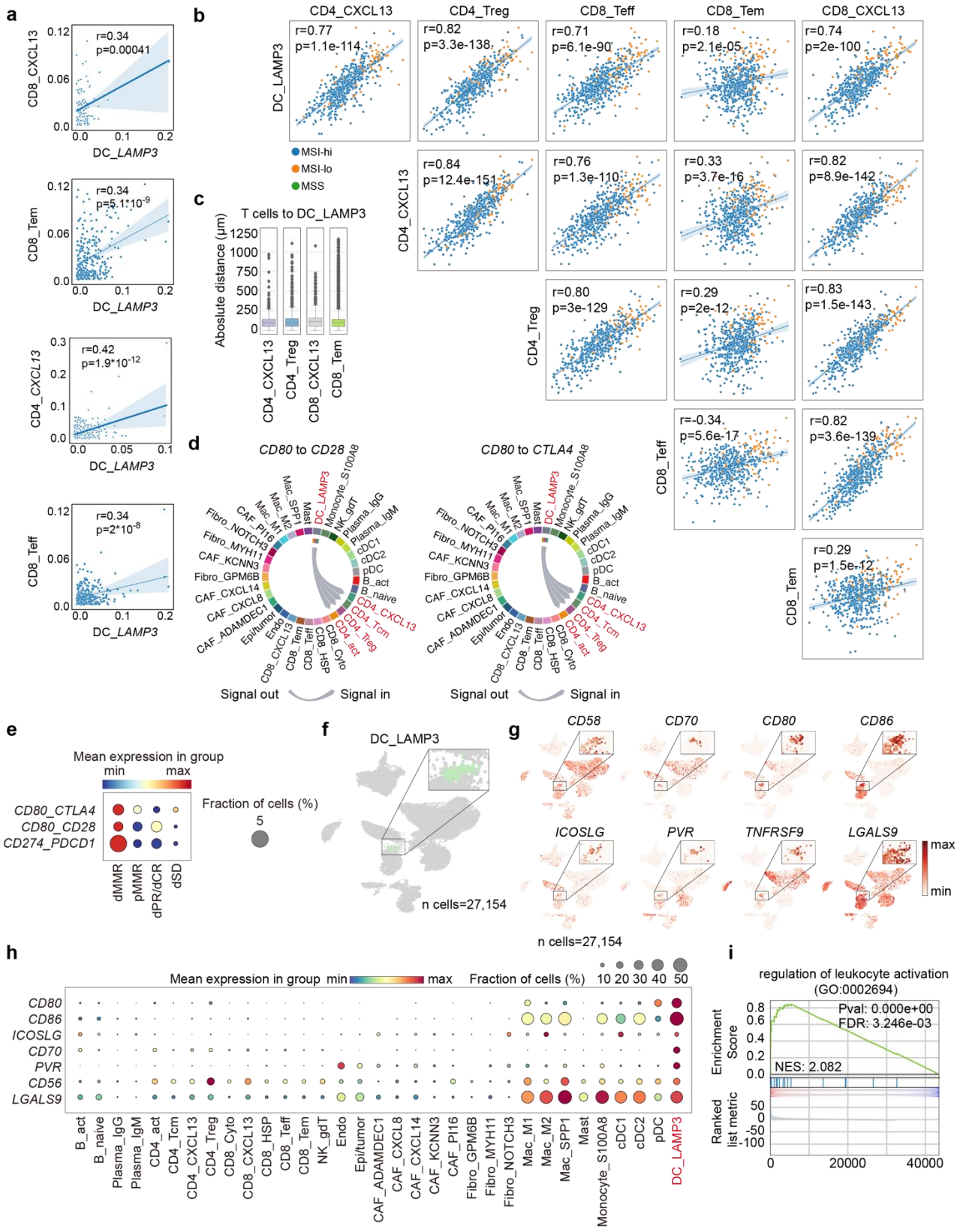
a
CD8_CXCL13
r=0.34
p=0.00041
DC_LAMP3
CD8_Tem
r=0.34
p=5.1*10-9
CD4_CXCL13
r=0.42
p=1.9*10-12
CD8_Teff
r=0.34
p=2*10-8
b
CD4_CXCL13
CD4_Treg
CD8_Teff
CD8_Tem
CD8_CXCL13
DC_LAMP3
r=0.77 p=1.1e-114
r=0.82 p=3.3e-138
r=0.71 p=6.1e-90
r=0.18 p=2.1e-05
r=0.74 p=2e-100
MSI-hi
MSI-lo
MSS
r=0.84 p=12.4e-151
r=0.76 p=1.3e-110
r=0.33 p=3.7e-16
r=0.82 p=8.9e-142
r=0.80 p=3e-129
r=0.29 p=2e-12
r=0.83 p=1.5e-143
r=-0.34 p=5.6e-17
r=0.82 p=3.6e-139
r=0.29 p=1.5e-12
c
T cells to DC_LAMP3
Absolute distance (μm)
d
CD80 to CD28
CD80 to CTLA4
Signal out
Signal in
e
Mean expression in group
min
max
CD80_CTLA4
CD80_CD28
CD274_PDCD1
Fraction of cells (%)
dMMR
pMMR
dPR/dCR
dSD
f
DC_LAMP3
n cells=27,154
g
CD58
CD70
CD80
CD86
ICOSLG
PVR
TNFRSF9
LGALS9
max
min
h
Mean expression in group min max
Fraction of cells (%)
CD80
CD86
ICOSLG
CD70
PVR
CD56
LGALS9
i
regulation of leukocyte activation
(GO:0002694)
Pval: 0.000e+00
FDR: 3.246e-03
NES: 2.082
Enrichment Score
Ranked list metric

Supplementary Figure 7. ***Key pathways in the potential interactions between DC_LAMP3 and T cell clusters in the tumor-stroma boundary.***

a Correlations of DC_*LAMP3* and T cell clusters in the Stereo-seq data from treatment naïve dMMR patients. Each scattered dot represents a single spatial bin. **b** Pearson correlation of the signature scores of DC_*LAMP3* and T cell clusters from MSI-hi (MSI score≥10, n = 78 patients) and MSI-lo (MSI score≥10, n = 494 patients) groups in COAD TCGA data are shown. The signature Z-scores are calculated using the top10 DEGs from each cell cluster in our scRNA-seq data. **c** The box and whisker plot shows the absolute distance of each T cell cluster to proximal DC_LAMP3. Data are represented as box-whisker plot (mean±IQR: 25%~75%) and analyzed by two-tailed unpaired Student-t test with Bonferroni correction. N cells: CD4_CXCL13=3,036, CD4_Treg=3,806, CD8_CXCL13=980, CD8_Tem=7,568. **d** The chord plots show the ligand-receptor interaction of *CD80_CD28* (left) and *CD80_CTLA4* (right) between DC_*LAMP3* and $CD4^+$T cell clusters. **e** Bubble plots of expression profiling of ligand-receptor pairs *CD80_CTLA4*, *CD80_CD28* and *CD274_PDCD1* in the tumor-stromal boundary of indicated patient groups are shown. The plots are sized by the fraction of cells with positive gene expression, while the color represents the gene expression level. **f** UMAP of DC_LAMP3 cluster and **g** its marker genes are shown. N cells=27,154; n samples: 5 pMMR, 2 dPR/CR, 3 dSD. **h** Bubble plots of the expressions of co-stimulatory and co-inhibitory ligands in the single cell clusters. The plot are sized by the fraction of cells with positive gene expression, while the color represents the gene expression level. **i** GSEA plot of the upregulated genes related to regulation of leukocyte activation (GO:0002694) in the tumor-stroma boundary of treatment naïve dMMR compared to pMMR patients.

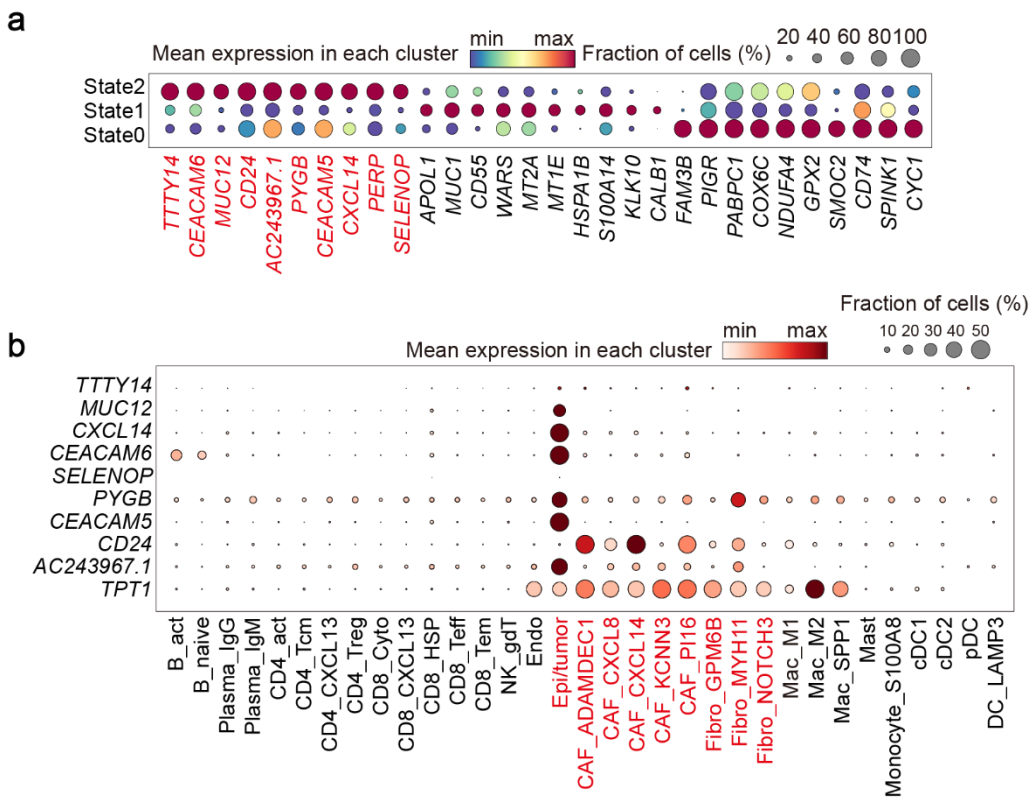
a
Mean expression in each cluster
min
max
Fraction of cells (%)
20 40 60 80100
State2
State1
State0
TTTY14
CEACAM6
MUC12
CD24
AC243967.1
PYGB
CEACAM5
CXCL14
PERP
SELENOP
APOL1
MUC1
CD55
WARS
MT2A
MT1E
HSPA1B
S100A14
KLK10
CALB1
FAM3B
PIGR
PABPC1
COX6C
NDUFA4
GPX2
SMOC2
CD74
SPINK1
CYC1
b
Fraction of cells (%)
Mean expression in each cluster
min
max
10 20 30 40 50
TTTY14
MUC12
CXCL14
CEACAM6
SELENOP
PYGB
CEACAM5
CD24
AC243967.1
TPT1
B_act
B_naive
Plasma_IgG
Plasma_IgM
CD4_act
CD4_Tcm
CD4_CXCL13
CD4_Treg
CD8_Cyto
CD8_CXCL13
CD8_HSP
CD8_Teff
CD8_Tem
NK_gdT
Endo
Epi/tumor
CAF_ADAMDEC1
CAF_CXCL8
CAF_CXCL14
CAF_KCNN3
CAF_PI16
Fibro_GPM6B
Fibro_MYH11
Fibro_NOTCH3
Mac_M1
Mac_M2
Mac_SPP1
Mast
Monocyte_S100A8
cDC1
cDC2
pDC
DC_LAMP3
c
CAF_PI16 to CAF_CXCL14
Pseudotime
0
2
4
6
IFIT3
ANXA2
FBN1
IGFBP6
PI16
CD34
C3
S1000A4
CXCR4
FOXF2
CXCL14
TMEM19
POSTN
COL4A5
PTCH1
MMP11
BMP4
MMP1
3
2
1
0
-1
-2
CAF_PI16
CAF_CXCL14
CAF_PI16 to CAF_CXCL8
Pseudotime
0
2
4
6
IFIT1
IFIT3
CD55
IGF2
TMP3
CADM3
SLPI
S100A4
PI16
CD34
IGFBP5
IGFBP6
CCL2
KRT19
CLDN1
SERPINB4
SERPINB2
MMP3
3
2
1
0
-1
-2
CAF_PI16
CAF_CXCL8

Supplementary Figure 8. ***The features of CAFs in the tumor-stroma boundary***.

a Bubble plots of the expressions of the top 10 genes (ranked by p-value) in each cell state or **b** the top 10 highlighted genes in state 0 in the single cell clusters. The plots are sized by the fraction of cells with positive gene expression, while the color represents the gene expression level. **c** Heatmaps of the pseudo-temporal expression patterns of the top 100 genes during the lineage 0 (CAF_P*I16* to CAF_*CXCL14*) or lineage 1 (CAF_*PI16* to CAF_*CXCL8*) differentiation. Genes of interests are labelled.

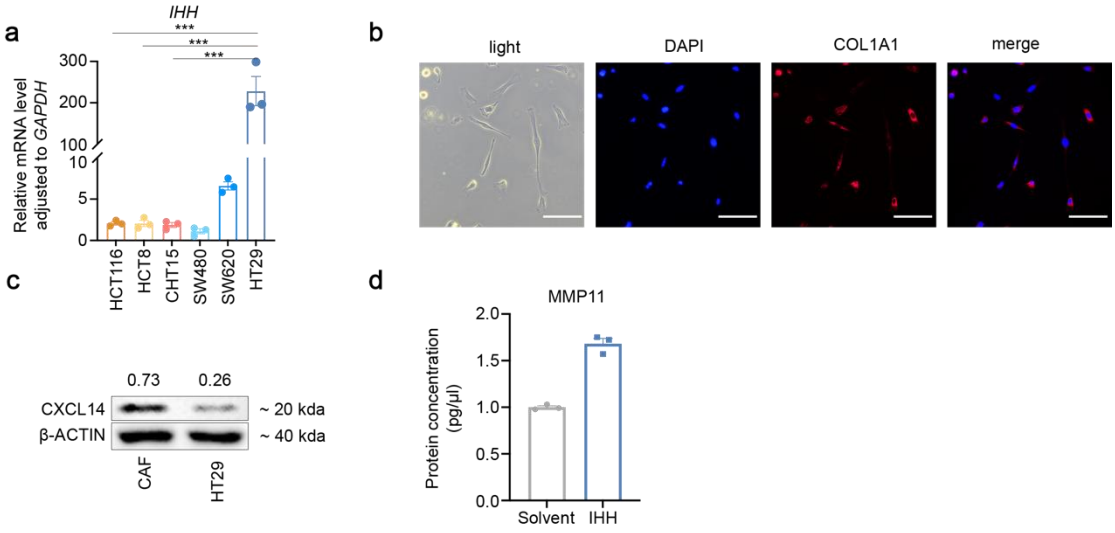

Supplementary Figure 9. ***MMP11 expression is upregulated by IHH in CXCL14^{+}CAF in vitro.***

a The relative expression of *IHH* to *GAPDH* in the 6 human CRC cell lines. Data are represented as mean±SD and analyzed by two-tailed unpaired Student-t test. N=3 independent experiment. **b** The representative images of the morphology and IF staining of COL1A1 in the CAFs are shown. DAPI was used as a positive control for cell nuclei staining. Scale bars, 20μm. **c** Western blot analysis of CXCL14 in CAF and HT29 cell lines is shown. β-actin serves as loading control. Number indicates the relative expression towards β-actin. This result represents 3 independent experimental repetitions. **d** The relative expression of *MMP11* to *GAPDH* in HT29 cells treated with PBS or IHH recombinant protein. Data are represented as mean±SD and analyzed by unpaired Student-t test. ***, $p<0.001$. N=3 independent experiment.